Applied Physics Letters

RESEARCH ARTICLE | OCTOBER 24 2005

Pressure-induced structural phase transition in $CaCrO_4$: Evidence from Raman scattering studies

Y. W. Long; W. W. Zhang; L. X. Yang; Y. Yu; R. C. Yu; S. Ding; Y. L. Liu; C. Q. Jin

Appl. Phys. Lett. 87, 181901 (2005)
https://doi.org/10.1063/1.2117624

AIP Publishing

Pressure-induced structural phase transition in $CaCrO_4$: Evidence from Raman scattering studies

Y. W. Long, W. W. Zhang, L. X. Yang, Y. Yu, R. C. Yu, S. Ding, Y. L. Liu, and C. Q. Jin[a)]
Institute of Physics, Chinese Academy of Sciences, Beijing 100080, People's Republic of China

(Received 25 May 2005; accepted 16 September 2005; published online 24 October 2005)

Raman spectroscopic studies have been carried out on $CaCrO_4$ under pressure up to 26.2 GPa at ambient temperature. The Raman spectra showed that $CaCrO_4$ underwent a continuous structural phase transition started near 6 GPa, and finished at about 10 GPa. It was found that the high-pressure phase could be quenched to ambient conditions. Pressure dependence of the Raman peaks suggested that there existed four pressure regions related to different structural characters. We discussed these characters and inferred that the nonreversible structural transition in $CaCrO_4$, most likely was from a zircon-type ($I4_1/amd$) ambient phase to a scheelite-type high-pressure structure ($I4_1/a$). © *2005 American Institute of Physics*. [DOI: 10.1063/1.2117624]

$CaCrO_4$ is an important cathode material in thermally activated electrochemical cells, and it also often be used in many industrial process as an intermediate compound formed in the system of Ca-Cr-O.[1–3] The thermodynamic properties of $CaCrO_4$, such as enthalpy, entropy, Gibbs free energy, heat capacity, and so on have been investigated in detail for the wide applications of $CaCrO_4$.[4–8] Temperature, chemical potential, and pressure are the three fundamental parameters to govern the thermodynamic state of materials. Traditionally temperature and chemical composition are the routine concerns of conventional materials. However, with the significant progress of high pressure technique, especially the breakthrough of integrated experimental methods based on diamond anvil cell (DAC), high pressure is gradually becoming a reachable physical dimension in modifying materials state. $CaCrO_4$ was conventionally regarded as a thermally stable material at the temperature even higher than 1000 °C, and its structural properties under high pressure were never reported in the literature as yet to our knowledge. It is known that Raman spectroscopy has been proved to be a convenient means to study structural characters of materials through the solid-state effects on the dynamical properties. Due to the development of DAC methods, high-pressure Raman spectroscopy has been available to investigate materials of pressure-related structural characters.[9,10] We present here for the first time a pressure-dependent Raman scattering study to detect the structural characters of $CaCrO_4$ under high pressure. We found the evidence of pressure-induced structural transition at 6 GPa, and analyzed different structural characters in four pressure regions. Furthermore, we concluded that the most likely structural transition route was from zircon-type to scheelite-type structure taking account of the available reports on other similar compounds.[11–14]

$CaCrO_4$ crystallizes into a zircon-type structure of tetragonal lattice with space group $I4_1/amd$ ($Z=4$) at ambient conditions. The structure of zircon-type $CaCrO_4$ is built from isolated and slightly distorted CrO_4 tetrahedral units, which are connected with CaO_8 dodecahedra by edge- and corner-sharing. The detailed structural description was discussed in Refs. 15 and 16. The highly pure $CaCrO_4$ polycrystalline powder used in this experiment was synthesized by conventional solid-state reaction method.[16] The powder sample was carefully loaded into a DAC with 500 μm culets. T301 stainless steel with a 250 μm hole and 300 μm thickness was used as gasket. 4:1 methanol-ethanol mixture was used as pressure medium. The pressure was calibrated by the ruby luminescence method.[17,18] The Raman spectra and the ruby luminescence were collected in the back-scattering geometry using a micro-Raman spectrometer (Jobin Yvon T64000) equipped with a charge-couple device (CCD) detector. A 25× microscope objective lens was used for focusing the laser beam and collection of the scattered light. The source for excitation was Verdi-2 solid-state laser (532 nm), and instrument resolution was 1 cm^{-1}.

Based on the point group analysis, we chose the phonons frequency range from 150 to 1000 cm^{-1} to detect the internal vibration of CrO_4 tetrahedra in $CaCrO_4$.[19] All of the Raman spectra in various pressures up to 26.2 GPa were shown in Figs. 1 and 2. Clearly the Raman peaks under different pressure are assigned in two frequency regions: 200–500 cm^{-1} and 800–1000 cm^{-1}, corresponding to O-Cr-O bending modes and Cr-O stretching modes in CrO_4 tetrahedra, respectively. At ambient pressure, six unambiguous Raman

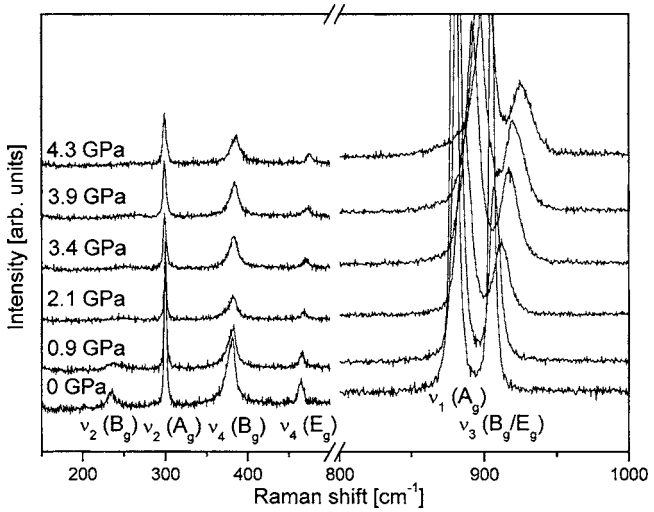

FIG. 1. Raman spectra of zircon-type $CaCrO_4$ in the pressure range from 0 to 4.3 GPa.

[a)]Author to whom correspondence should be addressed; electronic mail: cqjin@aphy.iphy.ac.cn

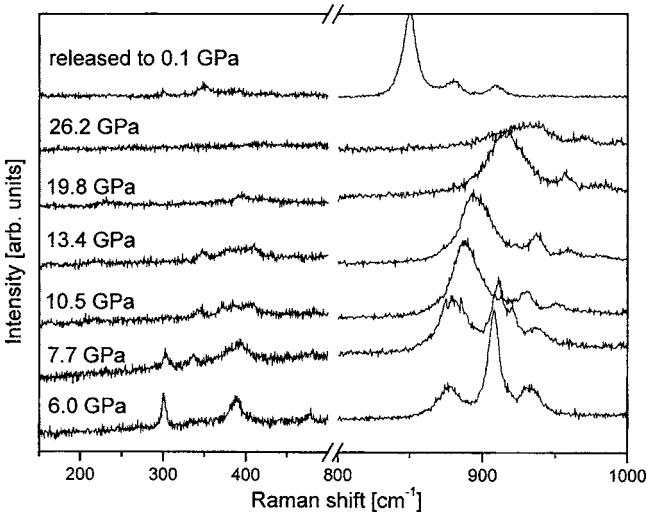

FIG. 2. Some representative Raman spectra that show the structural transition of $CaCrO_4$ in the pressure range from 6.0 to 26.2 GPa, and the irreversible character of this transition.

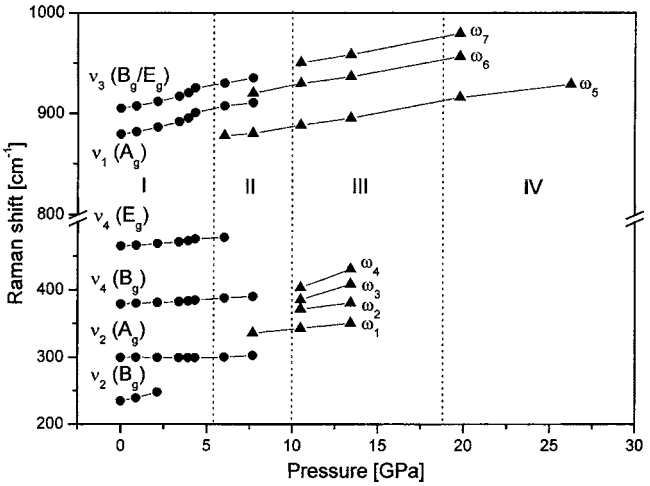

FIG. 3. Pressure dependence of the Raman peaks in $CaCrO_4$. Closed circles and triangles present the frequencies of Raman peaks at various pressures for zircon-type and new high-pressure phase, respectively. I–IV show the four different pressure regions related to different structural characters.

peaks were observed as reported in Ref. 20. According to the description of Ref. 19, the six Raman peaks were identified as $\nu_1(A_g)$, (symmetric-stretching modes), ν_3 (B_g and E_g), (antisymmetric-stretching modes), ν_2 (A_g and B_g), (symmetric-bending modes), and ν_4 (B_g and E_g), (antisymmetric-bending modes). The general rule is that ν_1 and ν_3 modes appear in a higher frequency region than ν_2 and ν_4 modes, and the intensity of the $\nu_1(A_g)$ peak is the strongest and the $\nu_2(B_g)$ peak the weakest.[19]

According to position shift and intensity change of Raman peaks with increasing pressure in 0–4.3 GPa as show in Fig. 1, it is clear that ν_1 and ν_3 peaks were more sensitive to pressure than ν_2 and ν_4 peaks. In this pressure range, both position and intensity were almost unchanged for ν_2 and ν_4 peaks, except for the gradually disappearance of ν_2 (B_g) peak when pressure reached 2.1 GPa. However, the shift of ν_1 and ν_3 peaks in the same pressure range was very obvious, and reached an average rate of 5.29 cm^{-1} GPa^{-1} and 5.22 cm^{-1} GPa^{-1}, respectively. Moreover, the intensity of ν_1 and ν_3 peaks, especially for ν_1 peak, decreased quickly with pressure raising. These indicate that pressure effect is more sensitive for Cr–O stretching modes than for O–Cr–O bending modes in zircon-type $CaCrO_4$. When pressure reached 6.0 GPa, a new Raman peak appeared at 878 cm^{-1} (marked with ω_5), and the intensity of other peaks distinctly declined accompanying with the broadening of ν_4 (B_g) peak, as showed in Fig. 2. Clearly, a new crystal structure has begun to appear at 6.0 GPa. When pressure continuously increased to 7.7 GPa, two other new Raman peaks were observed at 337 cm^{-1} (ω_1) and 920 cm^{-1} (ω_6), respectively, while ν_4 (A_g) peak vanished. In addition, the intensity of ν_2 (A_g), ν_1 (A_g), and ν_3 (B_g/E_g) peaks reduced quickly, and ν_4 (B_g) peak sequentially broadened, tending to split into two peaks. Apparently, two different kinds of crystal structure coexisted in the pressure range from 6.0 to 7.7 GPa in $CaCrO_4$. One crystal phase is the zircon-type structure, and the other is the new high-pressure phase, which we will discuss likely to be a scheelite-type structure in the following context. With pressure increasing to 10.5 GPa, ν_1 and ν_3 peaks vanished entirely and other two new peaks came forth at 372 cm^{-1} (ω_2) and 951 cm^{-1} (ω_7). At the same time, ν_4 (B_g) peak has split into two new peaks at 386 cm^{-1} (ω_3) and 404 cm^{-1} (ω_4). Heretofore, all the Raman peaks of zircon-type structure disappeared. This suggested the structural phase transition in $CaCrO_4$ under high pressure has been finished completely. With pressure further increasing until the highest 26.2 GPa reached in this experiment, no other new Raman peak was observed, except that Raman peaks of the high-pressure new phase become more broaden with increasing pressure. This is possibly an indication that the sample even trended to be amorphous at 26.2 GPa. Finally, we released the pressure to lowest (about 0.1 GPa) and found that the peaks of the high-pressure structure just remained in the Raman spectrum. Moreover, this character was unchanged 10 days later. This means that the phase transition started near 6 GPa is nonreversible and the high-pressure phase can be kept steadily as a metastable phase at ambient conditions.

From the pressure dependence of Raman peaks showed in Fig. 3, four pressure regions with different structural characters were observed for $CaCrO_4$ under high pressure. In region I there only existed the zircon-type structure. Cr–O stretching modes appeared more sensitive to pressure than O–Cr–O bending modes in this region. This was illustrated by the shift rate of phonons frequencies and intensity change of Raman peaks. The zircon-type and the new high-pressure structure coexisted in region II, which corresponded to the continuous structural transition process. New phase began to appear and became stronger and stronger with increasing pressure, while zircon-type structure became more and more faint and was gradually replaced by the new high-pressure phase in this region. In region III, zircon-type structure completely disappeared and only the peaks of the new high-pressure structure were present in the spectra. The intensity of Raman peaks in lower frequency region was feeble compared with high frequency region, but still discernable. In region IV, Raman peaks sharply broaden and the sample tended to be amorphous. These interesting structural characters at various pressure regions have been confirmed by our recent synchrotron radiation experiments.[21]

Now we discuss the phase relation with respect to pressure by comparison with RVO_4 (R=Y, Tb, and Dy) system. At ambient conditions, $CaCrO_4$ and RVO_4 have the same zircon-type crystal structure (tetragonal, z=4), space group

(No. 141, $I4_1/amd$), d electronic distribution ($3d^0 4s^0$ for V^{5+} and Cr^{6+}) as well as similar lattice parameters. Therefore, it is reasonable to expect a comparable high-pressure behavior of $CaCrO_4$ and RVO_4. Jayaraman *et al.* have studied the Raman spectra of RVO_4 under high pressure and found a nonreversible pressure-induced structural phase transitions from zircon-type to scheelite-type in RVO_4 based on zero-pressure x-ray diffraction (XRD) of the pressure-released sample.[11,12] Their analysis showed the symmetry declined and the space group transformed to $I4_1/a$ when the structural transition happened. Recently, Wang *et al.* testified the result of structural phase transition in YVO_4 using *in situ* high-pressure angle-resolved XRD.[13] It is the usual rule that there is an unambiguous decrease of V–O stretching modes frequencies with the transition from zircon-type to scheelite-type structure.[11,13] Therefore, as a result of this phase transition, some new Raman peaks should appear, whose frequencies are lower than the corresponding frequency of ν_1 (A_g), ν_3 (B_g), or ν_3 (E_g) peak. Considering our results, there was an observable decline of the Cr–O stretching modes frequencies when the structural phase transition happened, as shown in Figs. 2 and 3. For example, a new Raman peak (ω_5) appeared at 878 cm^{-1} at 6.0 GPa, which was visibly less than the frequency (911 cm^{-1}) of ν_1 (A_g) peak; another new Raman peak (ω_6) appeared at 920 cm^{-1}, which is also less than the frequency (936 cm^{-1}) of the degenerate ν_3 (B_g/E_g) peak. The appearance of these new Raman peaks indicated the change of Cr–O bond strength in CrO_4 tetrahedra. According to the expression for force constant κ: $\nu = \frac{1}{2}\pi\sqrt{\kappa/m}$ (ν and m are the vibrational frequency and renormalized mass ($1/m = 1/m_{Cr} + 1/m_O$), respectively), we estimated that the Cr–O bond strength decreased of 7% with the decline of Cr–O bond stretching frequency from 911 to 878 cm^{-1} when the structural phase transition started to happen at 6 GPa. This suggested that the Cr–O bond length would increase with the appearance of new phase, as observed in YVO_4 phase transition.[13] So we regarded that the density increase in the structural transition do not result from a volume reduction of CrO_4 tetrahedra, but from a more efficient packing of the coordination polyhedra and the elimination of a structural hole in the zircon-type $CaCrO_4$, as mentioned in Refs. 22 and 23. Accordingly, our Raman scattering results well agree with the characters of zircon-type to scheelite-type structural transition for RVO_4 system under high pressure. We, therefore, assign the new high-pressure phase in $CaCrO_4$ observed in our experiment to a scheelite-type structure with space group $I4_1/a$ (No. 88). Certainly, the accurate phase transition and the structural determination should be confirmed by careful analysis of the data of our recent investigation by high-resolution angle-resolved XRD under high pressure.

In conclusion, we investigated the pressure-dependent Raman scattering on $CaCrO_4$ in the pressure range 0–26.2 GPa at ambient temperature. A nonreversible high-pressure phase was observed at 6 GPa. The pressure dependence of Raman peaks showed a series of interesting structural transitions in $CaCrO_4$ under high pressure. We analyzed these pressure-related structural characters and assigned the phase transition route was from zircon- to scheelite-type structure accompanying with an increase of Cr–O bond length in CrO_4 tetrahedron.

This work was partially supported by the national nature science foundation of China (50328102, 50321101, and 50332020), the state key fundamental research project (2002CB613301), and Chinese Academy of Sciences.

[1] B. H. Van Domelen and R. D. Wehrle, Proc. 9th Intersoc. Energy Conversion Eng. Conf., The American Society of Mechanical Engineers, 1974.
[2] D. A. Nissen, J. Electrochem. Soc. **126**, 176 (1979).
[3] F. M. Delnick and D. K. McCarthy, J. Electrochem. Soc. **130**, 1875 (1983).
[4] R. P. Clark, P. K. Gallagher, and B. M. Dillard, Thermochim. Acta **33**, 141 (1979).
[5] T. G. Wang and Z. H. Li, J. Chem. Eng. Data **49**, 1300 (2004).
[6] Y. M. Lee and C. L. Nassaralla, Thermochim. Acta **371**, 1 (2001).
[7] K. T. Jacob, M. K. Kale, and K. P. Abraham, J. Electrochem. Soc. **139**, 157 (1992).
[8] A. M. Azad and O. M. Sreedharan, Thermochim. Acta **194**, 129 (1992).
[9] M. G. Pravica, Y. R. Shen, and M. F. Nicol, Appl. Phys. Lett. **84**, 5452 (2004).
[10] M. Kuball, J. M. Hayes, A. D. Prins, N. W. A. van Uden, D. J. Dunstan, Y. Shi, and J. H. Edgar, Appl. Phys. Lett. **78**, 724 (2001).
[11] A. Jayaraman, G. A. Kourouklis, G. P. Espinosa, A. S. Cooper, and L. G. Van Uitert, J. Phys. Chem. Solids **48**, 755 (1987).
[12] S. J. Duclos, A. Jayaraman, G. A. Kourouklis, A. S. Cooper, and R. G. Maines, J. Phys. Chem. Solids **50**, 769 (1989).
[13] X. Wang, I. Loa, K. Syassen, M. Hanfland, and B. Ferrand, Phys. Rev. B **70**, 064109 (2004).
[14] S. A. Miller, H. H. Caspers, and H. E. Rast, Phys. Rev. **168**, 964 (1968).
[15] B. G. Hyde and S. Andersson, *Inorganic Crystal Structures* (Wiley, New York, 1989).
[16] G. Weber and K. J. Range, Z. Naturforsch. **51b**, 751 (1996).
[17] G. J. Piermarini, S. Block, J. D. Barnett, and R. A. Forman, J. Appl. Phys. **46**, 2774 (1975).
[18] H. K. Mao, J. Xu, and P. M. Bell, J. Geophys. Res. **91**, 4673 (1986).
[19] A. Muller, E. J. Baran, and R. O. Carer, Struct. Bonding (Berlin) **26**, 81 (1976).
[20] Y. Aoki and H. Konno, J. Solid State Chem. **156**, 370 (2001).
[21] Y. W. Long *et al.* (to be published).
[22] V. S. Stubican and Z. Roy, Z. Kristallogr. **119**, 90 (1963); J. Appl. Phys. **34**, 1888 (1963).
[23] A. F. Reid and A. E. Ringwood, Earth Planet. Sci. Lett. **6**, 205 (1969).